Diffusion Tensor Imaging in Assessment of White Matter Micro-Structural Changes in Adult-Onset Idiopathic Focal Cervical Dystonia

Naglaa Samy Fahmy Abou Taira[a*], Shaimaa Gamal Eldeen Abd Elreheem Mahmoud[a], Sara Essam Hasby[a]

[a]Radiology Department, Faculty of Medicine, Tanta University, Tanta, Egypt

Abstract

Background: Diffusion tensor imaging (DTI) metrics include fractional anisotropy (FA) that allow estimating the directions of diffusion of water molecules so it can indicate the nerve fibers alignments and mean diffusivity (MD) that represents the overall magnitude of water diffusion and is mainly influenced by density of different cells as well as the extracellular space structure.

Objectives: To assess the added value of DTI using a ROI-based analysis as a quantitative evaluation of the white matter micro-structural changes among patients diagnosed with adult-onset idiopathic focal cervical dystonia.

Patients and methods: This prospective case-control study investigates the utility of diffusion tensor imaging (DTI) metrics fractional anisotropy (FA), mean diffusivity (MD), and apparent diffusion coefficient (ADC) in detecting microstructural white matter changes in adults with idiopathic focal cervical dystonia (AOIFCD). Forty-five patients with AOIFCD, their mean age was 40.51 ± 7.45 years, 14 of them were males (31.11%) and 31 were females (68.89%). Other twenty age and sex-matched healthy controls were enrolled in the study to compare their data with the diseased group, both groups underwent DTI on a 1.5T MRI scanner The study quantitatively compared DTI parameters across 17 brain regions, including both white and grey matter structures, and performed tractography of the corticospinal tracts (CST). Diagnostic performance was evaluated using ROC curve analysis.

Results: The diagnostic performance of the measured DTI parameters exhibited, as regard FA it demonstrated that the highest area under curve (AUC) was for FA at right putamen (0.995, $p<0.001$*), while as regard to the diagnostic performance of the measured MD, it demonstrated that the highest AUC was for MD at Cortico-Spinal Tract (CST) (1, $p<0.001$*), with sensitivity& specificity of 100 % both. Assessment of the diagnostic performance of the measured apparent diffusion coefficient (ADC) demonstrated that the highest AUC was for ADC at left cerebellar hemisphere, ADC at Corpus Callosum (CC) genu, ADC at CC splenium and ADC at CST (1, $p<0.001$*), with a sensitivity &specificity both of 100%.

Conclusion: The integration of quantitative DTI parameters across multiple white matter regions provides a robust framework for identifying microstructural changes in patients with adult-onset idiopathic focal cervical dystonia.

Keywords: Tensor Imaging; White Matter Micro-Structural; Adult-Onset Idiopathic; Focal Cervical Dystonia.

DOI: 10.21608/SVUIJM.2025.387915.2178

*Correspondence Naglaasamy86@gmail.com

Received: 22 May,2025.
Revised: 1 July, 2025.
Accepted: 7July, 2025.
Published: 9 July, 2025

Cite this article as Naglaa Samy Fahmy Abou Taira, Shaimaa Gamal Eldeen Abd Elreheem Mahmoud, Sara Essam Hasby.(2025). Diffusion Tensor Imaging in Assessment of White Matter Micro-Structural Changes in Adult-Onset Idiopathic Focal Cervical Dystonia. *SVU-International Journal of Medical Sciences*. Vol.8, Issue 2, pp: 197-211.

Introduction

Dystonia is a neurological condition that is characterized by involuntary muscle contractions that cause odd, repetitive movements or improper posture. It can happen by itself or in combination with other neurological symptoms. Dystonia is usually categorized as idiopathic, acquired, or inherited **(Albanese et al., 2013)**.

Gene mutations, which interfere with mechanisms including cellular signaling and the regulation of gene expression, are the most common cause of early-onset hereditary diseases **(Balint et al., 2018)**.

In contrast, acquired dystonia results from brain damage due to factors such as hypoxia, infection, autoimmune vasculitis, stroke, head injury, or exposure to toxic substances like certain drugs or heavy metals **(Jinnah and Sun, 2019; Sharma, 2019)**.

The key patho-physiological mechanisms involved in dystonia include disrupted inhibitory neural circuits, impaired synaptic plasticity, and sensory processing abnormalities **(Quartarone and Hallett, 2013)**.

Clinically, dystonia presents with a wide range of symptoms, and its phenotypic variability often makes it difficult to clearly associate with specific causes, particularly given the incomplete understanding of its underlying mechanisms. In individuals with dystonic cerebral palsy (DCP), imaging frequently reveals lesions in brain regions such as the thalamus, putamen and globus pallidus **(Krägeloh-Mann et al., 2002)**.

Diffusion tensor imaging (DTI) is a new MRI-based technique that enables the in vivo visualization of water molecule diffusion within different biological tissue. Although it is used more frequently to assess the white matter pathways integrity, it provides valuable insights into the features of deep gray matter regions micro-structural, shedding light on cellular organization and density within nuclei **(Vaillancourt et al., 2009)**. Key DTI metrics include both fractional anisotropy (FA) that allow estimating the directions of diffusion of water molecules so it can indicate the nerve fibers alignments and mean diffusivity (MD) that represents the overall magnitude of water diffusion and is mainly influenced by density of different cells as well as the extracellular space structure **(Lehéricy et al., 2013)**.

This study aimed to assess the added value of DTI using a ROI-based analysis as a quantitative evaluation of the white matter micro-structural changes among cases diagnosed with adult onset idiopathic focal cervical dystonia.

Patients and methods

This prospective case-control study included 45 patients suffering from adult-onset idiopathic cervical dystonia who were enrolled and followed up in the Neurology Department Tanta University Hospital from the period of 1st December 2024 to end of January 2025. Other 20 healthy control group of matched age and sex were enrolled in the study for comparison of their data with the diseased groups.

Inclusion criteria

Patients suffering from idiopathic cervical dystonia aged greater than 18 years (adult onset) were included in this study, they were diagnosed by an experienced neurologist in dystonia diagnosis. Besides, we included 20 healthy controls with the same age and sex matching, all of whom had normal brain MRIs upon visual inspection and no history of medical or neurological conditions.

Exclusion criteria

We excluded patients with childhood onset dystonia (history of dystonia starting before the age of eighteen , because childhood onset dystonia had a

generalized type representation), patients with organic brain problems like tumor, vascular lesion were ruled out from our study, in addition to cases taking medications causing dystonia , claustrophobic cases and those with MR contraindications including metallic device which are non-compatible with MRI , and patient with non MRI compatible cardiac pacemaker .Patients who refuse to perform the examination.

All participants underwent complete history taking, general assessment, and complete neurological assessment as well. Health controls were assessed to confirm lacking abnormal neurological findings.

This study was approved by the Medical Ethics Committee of Faculty of medicine, Tanta University. The ethical approval code is 36264PR1023/12/24. Written informed consent was obtained from all participants prior to imaging and data collection.

The severity of Dystonia was evaluated on the same day of the MRI scan via the use of the phenotype-specific Toronto Western Spasmodic Torticollis Rating Scale (TWSTRS) for cervical dystonia, administered by two neurologists specializing in movement disorders.

The age of the start of the disease onset and duration of it were documented for all participants. To exclude potential confounding effects of botulinum toxin, the assessment of all patients was done three months after their last botulinum injection. None of the patients received any other form of therapy.

MRI imaging acquisition

All cases and control volunteers were scanned on a GE Signa 1.5 T Magnetic Resonance Imaging system at Tanta University Radio diagnosis Department MRI unit, prior to scanning, removal of all metal objects was ensured and entered the MRI scanner head 1st in a supine position. Foam padding was used to reduce head movement, and a standard head coil was utilized.

The MRI protocol included the following parameters: 4 mm slice thickness, 256 × 256 matrix size, and a field of view (FOV) ranging from 220 to 240 mm. The imaging sequences acquired were:

Axial T1-weighted imaging (T1WI) with TR/TE = 300–600/10–30 m/s. Axial T2-weighted imaging (T2WI) with TR/TE = 700–2000/80–100 m/Axial and/or coronal oblique FLAIR with TR/TE/TI = 6000–8000/140/1400 ms. Diffusion-weighted imaging (DWI) with b-values of 0 and 1000. Susceptibility-weighted imaging (SWI).

DTI: A high-resolution 3D T1-weighted spoiled gradient echo pulse sequence was obtained with the following parameters: TR/TE/TI = 9.7/4.6/400 ms, flip angle (θ) of 35°, 124 slices with a thickness of 0.8 mm, a matrix of 208 × 170, FOV of 23 cm, and 260 contiguous sections. The total acquisition time was several minutes.

The DTI sequence was performed using spin echo-planar imaging protocol of a one shot with forty diffusion-encoding directions. The parameters included: TR equals 8,830 ms, TE equals 80 ms, acquisition matrix equals 112 × 110 mm, voxel size equals 2.00 × 2.03 × 2.00 mm, FOV dimensions of 224 mm (Rt–Lt), 224 mm (anteroposteriorly), and 120 mm (feet–head), and a reconstruction voxel size of 1.75 mm. The b-value was set at 800 mm/s, with a total of sixty slices acquired.

Data processing and analysis: The DTI data were transmitted to the workstation for post-processing. The images were converted into color-coded maps, from which different DTI metrics including FA, MD, and apparent diffusion coefficient (ADC) were derived.

A total of 17 regions of interest (ROIs) were selected within localized specific brain regions in both patients and

health controls. Equal sized circular ROIs were placed on specific white matter regions including the corpus callosum (genu, body, and splenium), the anterior and posterior limb of the IC, in as well as cerebellar subcortical white matter. Also we placed ROIs on specific gray matter regions including the basal ganglia (caudate , putamen and globus pallidus) thalamus, and supplementary motor area .

Regions of interest were initially identified on the FA maps and subsequently mapped onto the MD and ADC images to maintain accurate localization. The average diffusion parameter values for each ROI were thereafter documented.

DTI parameters for every region of interest (ROI) were measured and correlated with the values of relevant regions of interest in a healthy control group. The orientation and anatomical structure of the tracts were visualized using directionally encoded FA maps, where distinct colors represent fibers running along the 3 orthogonal planes.

The color-coded DTI maps were subjected to subjective evaluation through visual inspection in addition to objective evaluation through comparing FA, ADC, and MD value with those from the same sites in the control group

A 3D visualization of the bilateral cortico-spinal tracts (CST) was generated.
The biophysical tract characteristics (fiber density, FA, MD&ADC) were measured in both the patients and healthy control groups.
Every patient had a specific ID number, and all cases data was secret.

Statistical analysis

Statistical analysis was conducted using SPSS version 27 (IBM©, Armonk, NY, USA). Assessment of data distribution normality was done by using both Shapiro-Wilk test and histogram plots. For parametric quantitative variables, results are presented as mean ± standard deviation (SD), and group comparisons were performed using the unpaired Student's *t*-test. Qualitative variables were represented as frequencies and % and compared using the Chi-square test or Fisher's exact test. Receiver operating characteristic (ROC) curve analysis was employed to assess the diagnostic performance of tests. Statistical significance was defined as a two-tailed *p*-value <0.05, with hypotheses pre-specified to minimize bias.

Results

This prospective case-control study was done from first December 2024 to end of January 2025, after approval of our university ethical committee. All participants in this study provided written informed consent. Forty five patients diagnosed as adult-onset idiopathic focal cervical dystonia (AOIFCD) and 20 age- and sex -matched healthy controls were enrolled at this study. The participants were matched for age at assessment, their ages ranged from 20 to 45 years , with median age of the AOIFCD group 40.51 ± 7.45 years and 41.25 ± 6.8 for the control group ($p = 0.706$), as regard the patients 14 were men (31.11%)and 31 were women (68.89%) while the control groups included 5 men (25%) and 15 women (75%) . The median age at onset of dystonia was 30.2 ± 7.47 y and median time since dystonia was diagnosed 10.31 ± 5.43 y. All subjects were right-handed. The clinical criteria and demographic information of the studied groups are discussed in **(Table.1**), there was no significant difference detected among the studied groups.

Table 1. Patients' criteria of the studied groups

Variables		Patients (n=45)	Control (n=20)	P value
Age (y)		40.51 ± 7.45	41.25 ± 6.8	0.706
Sex	**Male**	14 (31.11%)	5 (25%)	0.617
	Female	31 (68.89%)	15 (75%)	
Duration of dystonia (years)		10.31 ± 5.43	-	-
Age of dystonia onset (years)		30.2 ± 7.47	-	-

Data are presented as mean ± SD or frequency (%).

The mean Fractional Anisotropy values of the ROIs of the studied patients were lower than that of the control groups, fractional anisotropy value was insignificantly different at right band left (caudate, globus pallidum, thalamus, internal capsule, cerebellar hemisphere, Supplementary motor area), as well as Corpus Callosum (CC) splenium between both groups. Fractional anisotropy value was significantly higher at right putamen and left putamen in patient's group in comparison to control group (P value <0.001) and was significantly lower at CC genu and CC body in patients than control (P value<0.001). (**Table.2**).

Table 2. Diffusion tensor imaging: fractional anisotropy values of the studied groups

Regions	Patients (n=45)	Control (n=20)	P value
Right caudate	0.15 ± 0.02	0.16 ± 0.02	0.063
Left caudate	0.14 ± 0.01	0.14 ± 0.02	0.156
Right putamen	0.19 ± 0.02	0.14 ± 0.02	**<0.001***
Left putamen	0.18 ± 0.03	0.15 ± 0.02	**<0.001***
Right globus pallidum	0.27 ± 0.02	0.26 ± 0.02	0.102
Left globus pallidum	0.23 ± 0.07	0.24 ± 0.05	0.748
Right thalamus	0.19 ± 0.04	0.21 ± 0.04	0.085
Left thalamus	0.24 ± 0.07	0.22 ± 0.04	0.330
Right internal capsule	0.59 ± 0.06	0.61 ± 0.05	0.292
Left internal capsule	0.61 ± 0.04	0.63 ± 0.04	0.061
Right cerebellar hemisphere	0.43 ± 0.08	0.47 ± 0.08	0.070
Left cerebellar hemisphere	0.45 ± 0.07	0.47 ± 0.08	0.387
Right SMA	0.12 ± 0.02	0.14 ± 0.04	0.064
Left SMA	0.15 ± 0.04	0.17 ± 0.03	0.094
CC genu	0.5 ± 0.09	0.61 ± 0.1	**<0.001***
CC body	0.48 ± 0.03	0.56 ± 0.08	**<0.001***
CC splenium	0.65 ± 0.03	0.64 ± 0.05	0.330

Data are presented as mean ± SD. *: Significant when P value ≤ 0.05. SMA: Supplementary motor area, CC: Corpus callosum.

As regards ADC values of the patients and controls there was insignificant difference between the 2 groups at right and left (caudate, putamen, globus pallidum, thalamus, internal capsule, Supplementary motor area) between both groups. The ADC

value was significantly higher at CC genu, body and splenium in patient's group in comparison to control group (P value <0.001) and was significantly lower at Rt & Lt cerebellar patient's group in comparison to control group (P value<0.001). (**Table.3**)

Table 3. Diffusion tensor imaging: ADC values of the studied groups

Regions	Patients (n=45)	Control (n=20)	P value
Right caudate	8.03 ± 0.57	8.26 ± 0.46	0.122
Left caudate	7.69 ± 0.47	7.92 ± 0.37	0.059
Right putamen	8.06 ± 0.35	8.24 ± 0.32	0.064
Left putamen	7.94 ± 0.36	7.83 ± 0.28	0.241
Right globus pallidum	8.71 ± 0.37	8.54 ± 0.38	0.094
Left globus pallidum	8.74 ± 0.37	8.59 ± 0.28	0.103
Right thalamus	8.72 ± 0.22	8.62 ± 0.17	0.060
Left thalamus	8.16 ± 0.4	7.98 ± 0.34	0.087
Right internal capsule	7.91 ± 0.7	8.13 ± 0.57	0.224
Left internal capsule	8.87 ± 0.32	8.77 ± 0.19	0.184
Right cerebellar hemisphere	7.02 ± 0.62	8.14 ± 0.32	**<0.001***
Left cerebellar hemisphere	6.64 ± 0.28	7.97 ± 0.33	**<0.001***
Right SMA	9.65 ± 0.31	9.53 ± 0.12	0.084
Left SMA	9.92 ± 0.26	9.81 ± 0.17	0.073
CC genu	8.48 ± 0.27	6.21 ± 0.49	**<0.001***
CC body	8.36 ± 0.76	6.99 ± 0.24	**<0.001***
CC splenium	9.89 ± 0.29	7.16 ± 0.58	**<0.001***

Data are presented as mean ± SD. *: Significant when P value ≤ 0.05. ADC: Apparent diffusion coefficient, SMA: Supplementary motor area, CC: Corpus callosum.

MD values of the two groups were insignificantly different at right and left (putamen, globus pallidum, thalamus, thalamus, internal capsule, cerebellar hemisphere, Supplementary motor area) as well as CC genu, body and splenium between both groups. MD value was significantly lower at Rt caudate, Lt caudate, Lt putamen and Lt globus pallidum in patients compared to control (P value<0.05). (**Table.4**)

Table 4. Diffusion tensor imaging: MD values of the studied groups

Regions	Patients (n=45)	Control (n=20)	P value
Right caudate	8.04 ± 0.62	8.82 ± 0.25	**<0.001***
Left caudate	7.57 ± 0.48	7.84 ± 0.26	**0.027***
Right putamen	8.19 ± 0.28	8.06 ± 0.22	0.069
Left putamen	7.6 ± 0.43	7.83 ± 0.26	**0.031***
Right globus pallidum	8.22 ± 0.52	7.98 ± 0.33	0.059
Left globus pallidum	8.4 ± 0.25	8.8 ± 0.35	**<0.001***
Right thalamus	8.63 ± 0.2	8.52 ± 0.24	0.062
Left thalamus	7.82 ± 0.54	7.96 ± 0.34	0.280
Right internal capsule	8.28 ± 0.75	8.08 ± 0.43	0.259
Left internal capsule	9.06 ± 0.68	9.14 ± 0.34	0.639
Right cerebellar hemisphere	6.95 ± 0.63	7.28 ± 1.08	0.131

Left cerebellar hemisphere	7.06 ± 0.39	7.34 ± 0.84	0.068
Right SMA	9.69 ± 0.27	9.55 ± 0.26	0.058
Left SMA	9.43 ± 0.35	9.33 ± 0.28	0.246
CC genu	8.03 ± 0.37	7.86 ± 0.27	0.063
CC body	7.6 ± 0.48	7.83 ± 0.28	0.053
CC splenium	5.96 ± 0.53	6.19 ± 0.48	0.110

Data are presented as mean ± SD. *: Significant when P value ≤ 0.05. MD: Mean diffusivity, SMA: Supplementary motor area, CC: Corpus callosum.

As regards Cortico-spinal tract FA and ADC showed significant decrease in patients compared with controls, while MD were significantly elevated in cases compared with control (P value<0.001). Fiber Tractography of the CST of the two groups revealed that fiber density affection showed significant increase in patients compared with controls (P value<0.001). 20 patients revealed affection of the right side & 25 patients showed left side affection. (**Table.5**)

Table 5. Diffusion tensor imaging of CST of the studied groups

Variables	Patients (n=45)	Control (n=20)	P value
FA at CST	0.31 ± 0.02	0.45 ± 0.08	**<0.001***
ADC at CST	6.87 ± 0.26	8.33 ± 0.19	**<0.001***
MD at CST	6.34 ± 0.2	8.16 ± 0.25	**<0.001***
CST fiber density affection	25 (55.56%)	0 (0%)	**<0.001***

Data are presented as mean ± SD. *: Significant when P value ≤ 0.05. FA: Fractional anisotropy, ADC: Apparent diffusion coefficient, MD: Mean diffusivity. CST: Corticospinal tract.

Assessment of the diagnostic performance of diffusion tensor imaging (DTI) parameters demonstrated that Fractional anisotropy can significantly predict changes in white matter micro-structural at right putamen, left putamen, CC genu, CC body and CST (P value<0.05) with highest prediction at CST at cut off ≤0.33 . (**Fig.1A**)

ADC can significantly predict changes in white matter micro-structural at right cerebellar hemisphere, left cerebellar hemisphere, CC genu, CC body, CC splenium, and CST (P value<0.05) with highest prediction at left cerebellar hemisphere, CC genu, CC splenium, and CST at cut off (≤7, >6.9, >7.9 and ≤7 respectively) .(**Fig.1B**)

MD can significantly predict changes in white matter micro-structural at RT caudate, Lt caudate, Lt putamen Lt globus pallidum and CST (P value<0.05) with highest prediction at CST at cut off ≤ 6.7 . (**Fig.1 C**)

The diagnostic performance of the measured DTI parameters exhibited , as regard FA it demonstrated that the highest AUC was for FA at right putamen (0.995, p<0.001*), in which an FA value exceeded 0.16 at the Rt putamen region was capable of detecting changes of the white matter micro-structure with a sensitivity of 86.67 % and a specificity of 75 % , while as regard to the diagnostic performance of the measured MD, it demonstrated that the highest AUC was for MD at CST (1, p<0.001*), in which an MD value of ≤6.7 at the CST region with sensitivity& specificity of 100 % both. Assessment of the diagnostic performance of the measured ADC demonstrated that the highest AUC was for ADC at left cerebellar hemisphere, ADC at CC genu, ADC at CC splenium and ADC at CST (1, p<0.001*), in which a value of ≤7, >6.9, >7.9 and≤7.2 at the region of the ADC at left cerebellar hemisphere, ADC at CC genu, ADC at CC

splenium and ADC at CST with a sensitivity &specificity of 100% both (**Table.6**).

Table 6. Diagnostic performance of FA, ADC and MD across different brain regions

Parameter	Cut-off	Sensitivity	Specificity	PPV	NPV	AUC	P value
FA at right putamen	>0.16	86.67%	75%	88.6%	71.4%	0.995	**<0.001***
FA at left putamen	>0.15	71.11%	55%	75.5%	50%	0.756	**<0.001***
FA at CC genu	≤0.61	84.44%	50%	79.2%	58.8%	0.776	**<0.001***
FA at CC body	≤0.49	71.11%	70 %	84.2%	51.9%	0.792	**<0.001***
FA at CST	≤0.33	86.67%	95 %	97.5%	76%	0.989	**<0.001***
ADC at right cerebellar hemisphere	≤7.5	80%	90%	94.7%	66.7%	0.951	**<0.001***
ADC at left cerebellar hemisphere	≤7	100%	100%	100%	100%	1.000	**<0.001***
ADC at CC genu	>6.9	100%	100%	100%	100%	1.000	**<0.001***
ADC at CC body	>7.4	95.56%	100%	97.8%	100%	0.999	**<0.001***
ADC at CC splenium	>7.9	100%	100%	100%	100%	1.000	**<0.001***
ADC at CST	≤7.2	100%	100%	100%	100%	1.000	**<0.001***
MD at right caudate	≤8.5	73.33%	75%	86.8%	55.6%	0.852	**<0.001***
MD at left caudate	≤7.9	77.78%	45%	76.1%	47.4%	0.652	**0.025***
MD at left putamen	≤7.6	57.78%	75%	83.9%	44.1%	0.667	**0.011***
MD at left globus pallidum	≤8.6	86.67%	60 %	83%	66.7%	0.808	**<0.001***
MD at CST	≤6.7	100%	100%	100%	100%	1.000	**<0.001***

PPV: positive predictive value, NPV: negative predictive value, AUC: area under the curve.

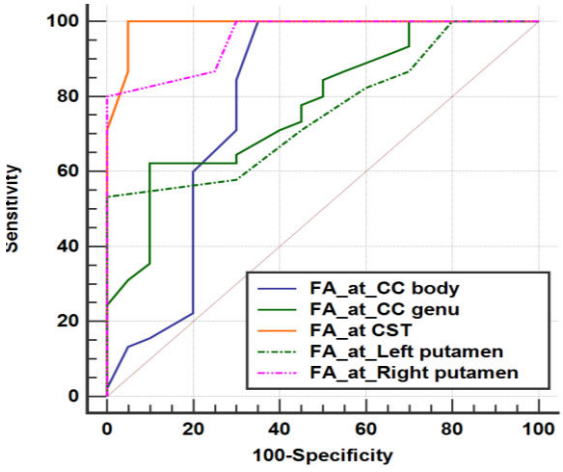

(A)

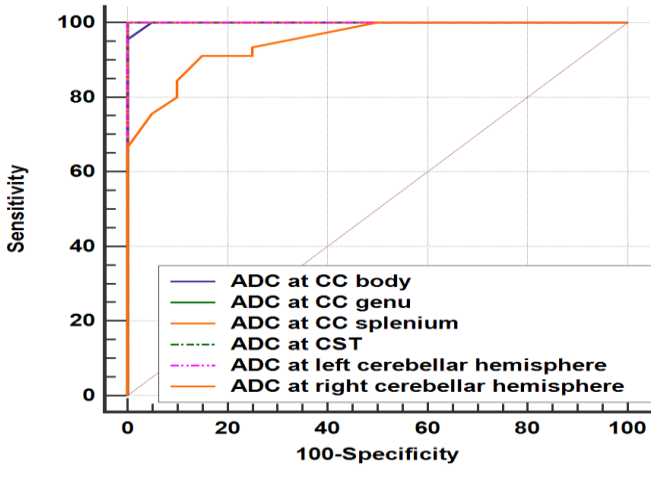

(B)

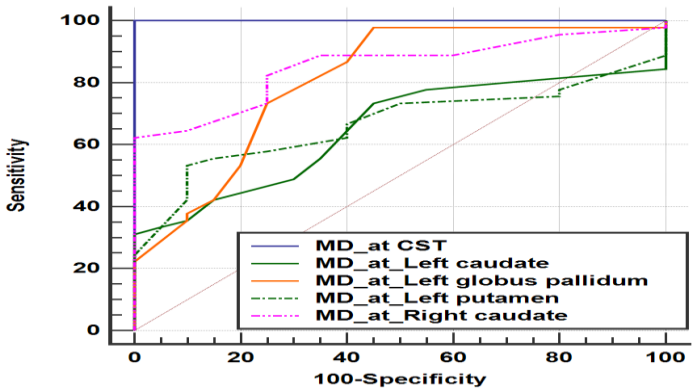

(C)

Fig.1. ROC curve of (A) fractional anisotropy, (B) ADC and (C) MD across different brain regions

Case 1: A 31-year-old male patient diagnosed with adult-onset cervical dystonia, complaining from neck pain & torticollis. (**Fig.2**)

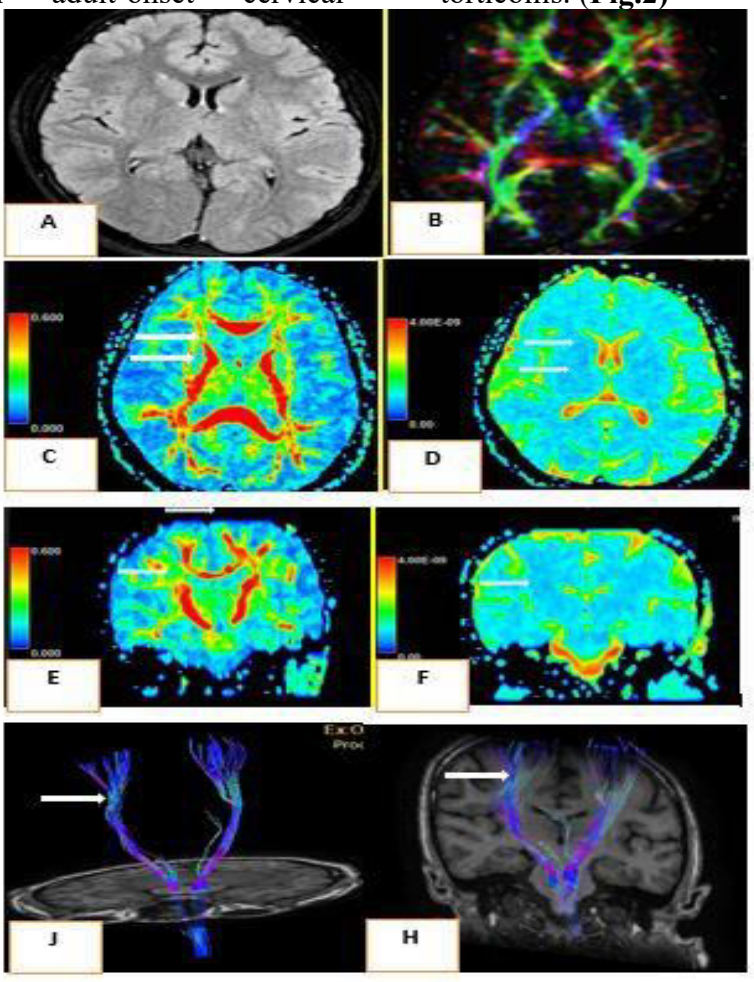

Fig.2 . A 31-year-old male patient diagnosed with adult-onset cervical dystonia, complaining from neck pain & torticollis .The conventional axial FLAIR MRI image (A) appears normal and shows no significant abnormalities. The directionally encoded color

map in the axial plane (B) displays the orientation of white matter fiber tracts: red indicates transverse, blue represents cranio-caudal, and green denotes antero-posterior directions. . Axial FA map(C) revealed focal decrease in the FA value in right Caudate nucleus & Putamen (white arrows) measuring about .14 & 0.19 respectively , while axial MD map (D) revealed focal increase in the MD values in the same regions measuring 7.5 & 7.6 respectively .Coronal FA map(E) revealed focal decrease in the FA value in right Cortico-spinal Tracts (CST) measuring 0.3 (white arrows) .Coronal MD map(F) revealed focal increase in the MD value in the same measuring 6.3 . Directionally encoded fiber tractography maps of both Corticospinal Tracts (J&H)revealed affected right sided CST showing mild fiber attenuation , in comparison to left sided CST(white arrows).

Case 2: A 30-year-old female patient with adult-onset cervical dystonia complaining from head dystonic tremors and neck stiffness. **(Fig.3)**

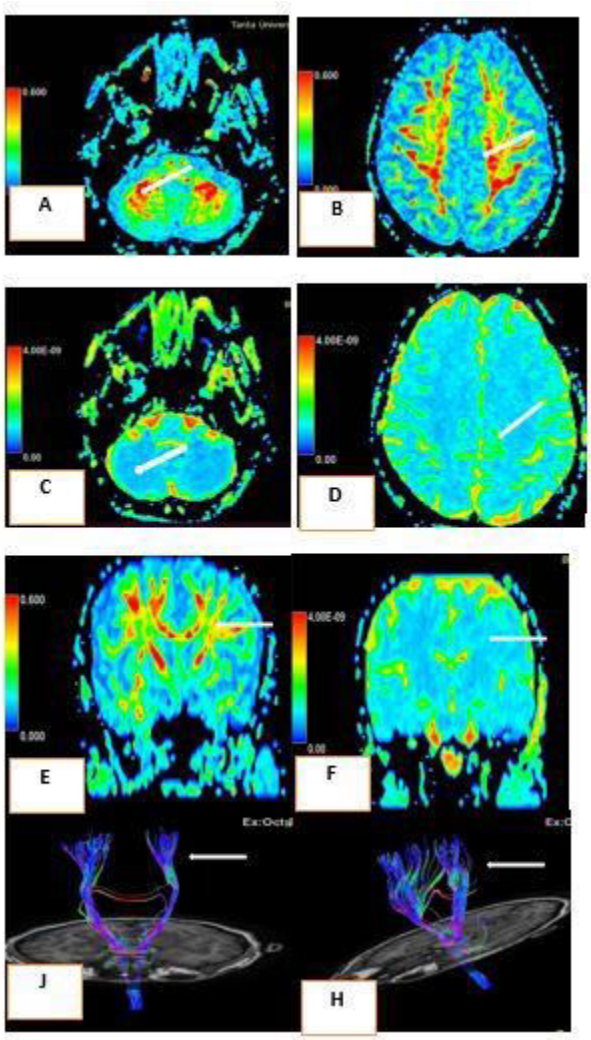

Fig.3.Axial FA maps(A & B) revealed focal decrease in the FA value in the sub-cortical white matter of the right cerebellar hemisphere (A) measuring 0.4 & supplementary motor area (SMA) measuring 0.14 (white arrows) (B). Axial MD map (C & D) revealed

focal increase in the MD value in the same regions (white arrows) measuring 6.9 & 9.7 respectively .Coronal FA map (E) revealed focal decrease in the FA value in left Cortico-spinal Tracts (CST) measuring 3.2 (white arrows) .Coronal MD map(F) revealed focal increase in the MD values in the same region measuring 6.3 .Directionally encoded fiber tractography maps of both Corticospinal Tracts (J&H) revealed affected left sided CST showing mild fiber attenuation, in comparison to right sided CST(white arrows).

Case 3: A 36-year-old female patient diagnosed to have adult-onset cervical dystonia, with involuntary muscle contractions of the neck. (**Fig.4)**

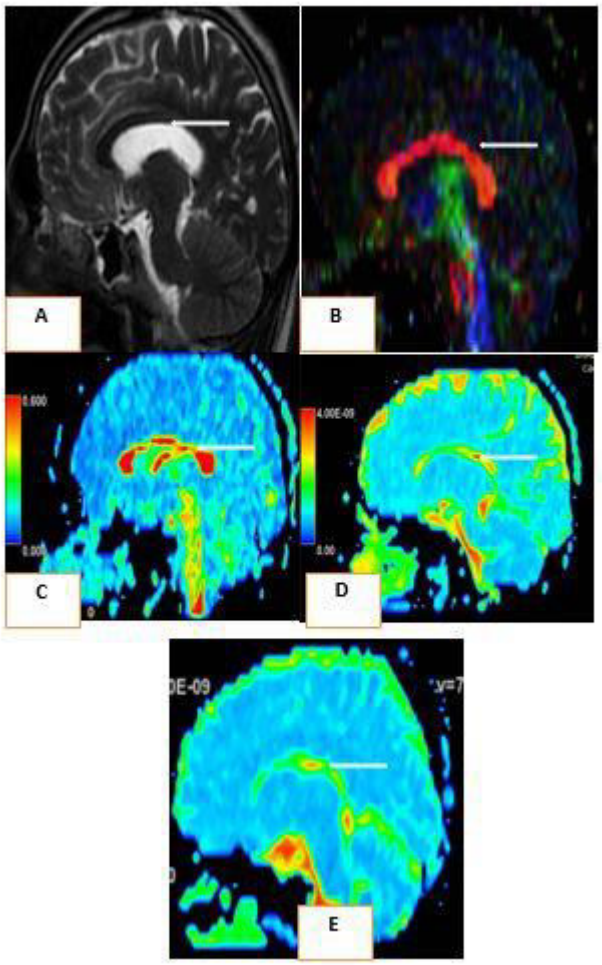

Fig.4. A 36 years old female patient diagnosed to have adult-onset cervical dystonia, with involuntary muscle contractions of the neck.conventional MR Sagittal T2WI image (A) appear normal and unremarkable . Sagittal directionally encoded color map(B) revealed red colour of Corpus Callosum . Sagittal FA map(C) revealed focal decrease in the FA value in the body of Corpus Callosum (measuring 0.35)(white arrows). Sagittal MD map (D) revealed focal increase in the D value in the body of corpus callosum measuring 0.76 (white arrows).Sagittal ADC map (E) revealed focal increase in the ADC value in the body of corpus callosum measuring 0.87 (white arrows).

Discussion

Dystonia's are one of the hyperkinetic movement disorders marked by persistent or intermittent muscle contractions that lead to abnormal movements and postures which are often repetitive. It can be categorized as either primary (idiopathic or genetic) or secondary, and its anatomical distribution may be focal, segmental, multifocal, or generalized. Adult onset idiopathic focal cervical dystonia (AOIFCD)is the most common form of adult-onset idiopathic dystonia **(di Biase et al., 2022)**.

In AOIFCD, excessive activity of cervical muscles and disrupted coordination lead to abnormal head and neck postures, often accompanied by pain and, in some cases, head tremor **(Giannì et al., 2023)**.

The pathophysiological mechanisms underlying AOIFCD remain poorly understood, contributing to a significant unmet clinical need. **(MacIver et al., 2024)**. Diagnosis is primarily clinical, depends on patient history and complete neurological examination. Functional and structural neuro-imaging studies have revealed both regional brain activation and anatomical alterations in individuals with cervical dystonia **(Luo et al., 2024)**.

Diffusion Tensor Imaging (DTI) is a new MRI technique which can detect subtle changes in white matter fibers, identifies changes in the extent of ADC and directionality FA of proton diffusion. These changes indicate alterations in tissue micro-structure and fiber organization. **(Fabbrini et al., 2008)**.

This study aimed to evaluate the added value of DTI using a ROI-based analysis as a quantitative evaluation of the white matter micro-structural changes to assess whether difference in network architecture and microstructural integrity is detected among cases diagnosed with primary dystonia and unaffected control.

To our knowledge, this is the first Egyptian study to examine the diagnostic accuracy of three DTI-derived quantitative parameters FA, MD, and ADC in patients with AOIFCD.

Indeed, DTI is a sophisticated MRI technique that utilizes the random movement of water molecules to generate detailed imaging data. This innovative neuroimaging method has enabled researchers to investigate the complex structural organization of the brain **(Ranzenberger et al., 2025)**.

In our study we found increased Fractional anisotropy value at bilateral putamen of basal ganglia while decreased mean diffusivity values at both caudate, Lt putamen and Lt globus pallidum in patients than control , That was in line with previous studies by Colosimo et al. **(Colosimo et al., 2005)** who documented increased FA in the putamen in patients with cervical dystonia in comparison with healthy controls and Fabbrini et al. **(Fabbrini et al., 2008)** who reported reduced MD in other basal ganglia regions .

Noteworthy, our results lend credence to the idea that support that basal ganglia connections have a significant part in the etiopathology of cervical dystonia, that was consistent with the study of Giannì C et al.**(Giannì C et al ., 2023)** who observed the increasing evidence of microstructural damage of several brain regions belonging to specific circuits, such as the basal ganglia-thalamo-cortical circuit, which likely reflects a common pathophysiological mechanism of focal dystonia . Also, previous volumetric MRI studies revealed evidence that there is volumetric abnormalities in putamen and globus pallidus of the CD cases **(Wang et al., 2025)**.

We identified reduced FA and elevated mean diffusivity (MD) in the genu and body of the corpus callosum in cervical

dystonia (CD) patients. These findings align with prior work by Fabbrini et al. **(Fabbrini et al., 2008)**, who reported significant regional FA differences in the corpus callosum between CD patients and controls. The observed FA reduction may reflect diminished axonal connectivity between cortical regions of the two hemispheres, potentially due to fewer callosal fibers. Such structural alterations could underlie disrupted motor cortical excitability in dystonia, providing a plausible mechanism for the aberrant motor activity characteristic of focal dystonia **(Berardelli et al., 1998)**.

As regard to ADC values ,our study revealed that ADC values were significantly higher at CC genu, CC body and CC splenium in patients with CD and was significantly lower at both cerebellar hemispheres also, these findings was coherent with results of Prell et al. **(Prell et al., 2013)** who determined reduced ADC in the putamen of cases with dystonia.

In the current study we had a detailed study of the Cortico-spinal tract DTI parameters, and we concluded that FA and ADC were significantly decreased in patients than control group, while MD values were significantly higher.

Fiber tractography of the CST of the two groups were done and revealed that fiber affection was significantly elevated in cases with CD in comparison with control groups , and these findings supports those of Sarin et al. **(Sarin et al., 2023)**, who proposed that the etiology of dystonia may result from impaired neural communication along corticospinal (pyramidal) and extrapyramidal motor pathways. This network-level disruption may underline the heterogeneous pathophysiology observed in dystonia.

Furthermore, our results of decreased FA and elevated MD, and ADC of the CST with fiber tract density affection in patients with CD lend credence to the idea that CST micro-structural affection or dysfunction may contribute to abnormal motor control, potentially influencing dystonic symptoms due to higher cortico-spinal excitability, even partly, This increased excitability may be a sequence of muscle spasm for long duration. A possible explanation underlying this heightened excitability could involve caudate and putamen lesions disrupting thalamocortical signaling pathways, particularly in the presence of preexisting deficits in intracortical inhibition. These findings are largely consistent with the model proposed by Trompetto et al. **(Trompetto et al., 2012)** which implicates network-level dysregulation in dystonia pathophysiology.

Limitations: This study was limited by the sample size as the relatively small sample size might limit the generalization of our results, so we emphasized the need for larger cohorts to validate the results and to better understand the variability within the CD population, also the difficulty in conclusively differentiating between causative factors and resultant effects observed in our DTI data as the observed microstructural changes may either contribute to or result from the pathophysiology of CD.

In summary, while DTI offers a powerful tool for exploring microstructural alterations in cervical dystonia, we must carefully consider these limitations. Addressing factors such as sample size, complex relationship between observed changes and disease pathology is essential for advancing our understanding of CD through neuroimaging studies.

Future studies should incorporate longitudinal designs with larger, multi-center cohorts to enhance statistical power and generalizability, and longer duration in order to confirm our findings.

Conclusion

The integration of quantitative DTI parameters (fractional anisotropy, mean diffusivity and apparent diffusion coefficient) across multiple white matter regions provides a robust framework for identifying microstructural changes in patients with AOIFCD. This multimodal approach enhances diagnostic precision and clarifies the neuroanatomical basis of motor network dysfunction in dystonia.

References

- **Albanese A, Bhatia K, Bressman SB, Delong MR, Fahn S, Fung VS, et al. (2013)**. Phenomenology and classification of dystonia: a consensus update. Mov Disord, 28(7): 863-873.
- **Balint B, Mencacci NE, Valente EM, Pisani A, Rothwell J, Jankovic J, et al. (2018)**. Dystonia. Nat Rev Dis Primers, 4(1): 25.
- **Berardelli A, Rothwell JC, Hallett M, Thompson PD, Manfredi M, Marsden CD. (1998)**. The pathophysiology of primary dystonia. Brain, 121 (Pt 7)1195-1212.
- **Colosimo C, Pantano P, Calistri V, Totaro P, Fabbrini G, Berardelli A. (2005)**. Diffusion tensor imaging in primary cervical dystonia. J Neurol Neurosurg Psychiatry, 76(11): 1591-1593.
- **di Biase L, Di Santo A, Caminiti ML, Pecoraro PM, Di Lazzaro V. (2022)**. Classification of Dystonia. Life (Basel), 12(2).
- **Fabbrini G, Pantano P, Totaro P, Calistri V, Colosimo C, Carmellini M, et al. (2008)**. Diffusion tensor imaging in patients with primary cervical dystonia and in patients with blepharospasm. Eur J Neurol, 15(2): 185-189.
- **Giannì C, Piervincenzi C, Belvisi D, Tommasin S, De Bartolo MI, Ferrazzano G, et al. (2023)**. Cortico-subcortical white matter bundle changes in cervical dystonia and blepharospasm. Biomedicines, 11(3): 753.
- **Jinnah H, Sun YV. (2019)**. Dystonia genes and their biological pathways. Neurobiology of disease, 129159-168.
- **Krägeloh-Mann I, Helber A, Mader I, Staudt M, Wolff M, Groenendaal F, et al. (2002)**. Bilateral lesions of thalamus and basal ganglia: origin and outcome. Dev Med Child Neurol, 44(7): 477-484.
- **Lehéricy S, Tijssen MA, Vidailhet M, Kaji R, Meunier S. (2013)**. The anatomical basis of dystonia: current view using neuroimaging. Mov Disord, 28(7): 944-957.
- **Luo Y, Liu H, Zhong L, Weng A, Yang Z, Zhang Y, et al. (2024)**. Regional structural abnormalities in thalamus in idiopathic cervical dystonia. BMC Neurol, 24(1): 174.
- **MacIver CL, Jones D, Green K, Szewczyk-Krolikowski K, Doring A, Tax CMW, et al. (2024)**. White matter microstructural changes using ultra-strong diffusion gradient mri in adult-onset idiopathic focal cervical dystonia. Neurology, 103(4): e209695.
- **Prell T, Peschel T, Köhler B, Bokemeyer MH, Dengler R, Günther A, et al. (2013)**. Structural brain abnormalities in cervical dystonia. BMC Neuroscience, 14(1): 123.
- **Quartarone A, Hallett M. (2013)**. Emerging concepts in the physiological basis of dystonia. Mov Disord, 28(7): 958-967.
- **Ranzenberger LR, Das JM, Snyder T. (2025)**. Diffusion Tensor Imaging. *StatPearls*. Treasure Island (FL): StatPearls Publishing

- **Sarin S, Lawal T, Abboud H. (2023)**. Spinal dystonia and other spinal movement disorders. Dystonia, 211303.
- **Sharma N. (2019)**. Neuropathology of Dystonia. Tremor Other Hyperkinet Mov (N Y), 9569.
- **Trompetto C, Avanzino L, Marinelli L, Mori L, Pelosin E, Roccatagliata L, et al. (2012)**. Corticospinal excitability in patients with secondary dystonia due to focal lesions of the basal ganglia and thalamus. Clin Neurophysiol, 123(4): 808-814.
- **Vaillancourt DE, Spraker MB, Prodoehl J, Abraham I, Corcos DM, Zhou XJ, et al. (2009)**. High-resolution diffusion tensor imaging in the substantia nigra of de novo Parkinson disease. Neurology, 72(16): 1378-1384.
- **Wang ZY, Chen F, Sun HH, Li HL, Hu JB, Dai ZY, et al. (2025)**. No reliable gray matter alterations in idiopathic dystonia. Front Neurol, 161510115.